Magnetic phase diagram and magnetic structure of $Gd(Sn_{1-x}In_x)_3$

C. L. Lin, T. Yuen, and T. Mihalisin
Department of Physics, Temple University, Philadelphia, Pennsylvania 19122
(Received 10 April 1996)

We have carried out measurements of the magnetic susceptibility, Mössbauer spectra, and specific heat on $Gd(Sn_{1-x}In_x)_3$. We observe an oscillatory variation of the antiferromagnetic transition temperature T_{N1} across the series from $GdSn_3$ ($x=0.0$) to $GdIn_3$ ($x=1.0$). For the range of In concentrations $0.265 \leqslant x \leqslant 0.565$, we find a second magnetic transition, at a temperature T_{N2} well below T_{N1}. These measurements along with the temperature dependence of ^{119}Sn Mössbauer spectra indicate that the ground-state magnetic structure is a type-I antiferromagnetic ordering for the Sn-rich side ($0 \leqslant x \leqslant 0.25$) and is a type-II for the very rich In side ($x \rightarrow 1.0$). For the range of In concentrations $0.265 \leqslant x \leqslant 0.565$ the magnetic structure is also of type I in the temperature interval $T_{N2} < T < T_{N1}$. The magnetic structure for $0.265 \leqslant x \leqslant 0.565$ with $T < T_{N2}$ and also for $0.565 < x < 1.0$ with $T < T_{N1}$ could be a canted antiferromagnetic ordering state. [S0163-1829(96)02637-9]

INTRODUCTION

Rare-earth and actinide based RSn_3 and RIn_3 systems and their pseudobinary alloys $R(Sn_{1-x}In_x)_3$ have attracted a great deal of interest over the past two decades[1–7] because of their salient features such as valence fluctuations, magnetic to nonmagnetic transitions, magnetic moment formation, and the presence of various magnetic structures. However, some of these features were found to be complicated and are not fully understood. To better understand such features it seems natural to study a simpler system. $Gd(In_{1-x}Sn_x)_3$ is an unique candidate for this purpose because Gd^{3+} has a half-filled $4f$ shell, $J=S=7/2$ (no orbital moment), and a large magnetic moment. Our previous studies[8] of the magnetic susceptibility of $Gd(Sn_{1-x}In_x)_3$ showed that $GdSn_3$ and $GdIn_3$ are both antiferromagnets with T_N's of 31 and 46 K, respectively. These results are consistent with those published by other groups.[1,9] We also observed an oscillatory variation of the antiferromagnetic transition temperature T_{N1} across the series, i.e., $0 \leqslant x \leqslant 1$, and a second magnetic transition T_{N2} at lower temperatures for some In-doped samples. In the present work we have extended the magnetic-susceptibility measurements to carefully determine the magnetic phase diagram. In addition, we have carried out measurements of the temperature dependence of the specific heat and Mössbauer spectra across the $Gd(Sn_{1-x}In_x)_3$ system. Our specific-heat and Mössbauer results exhibit a similar T_{N1} variation across the series, as well as the presence of the second magnetic transition T_{N2} in the range of In concentrations $0.265 \leqslant x \leqslant 0.565$, as was seen in the previous magnetic-susceptibility measurements. From these studies we infer that the magnetic structure changes from type-I antiferromagnetic ordering on the Sn-rich side ($0 \leqslant x \leqslant 0.25$) to type-II antiferromagnetic ordering on the very rich In side ($x \rightarrow 1.0$). For the range of In concentrations $0.265 \leqslant x \leqslant 0.565$, at $T_{N2} < T < T_{N1}$, the magnetic structure is also of type I. The magnetic structure for In concentrations $0.265 \leqslant x \leqslant 0.565$ with $T < T_{N2}$ and for $0.565 < x < 1.0$ with $T < T_{N1}$ could be a canted antiferromagnetic ordering state.

EXPERIMENTAL

Polycrystalline $Gd(Sn_{1-x}In_x)_3$ samples with $0 \leqslant x \leqslant 1$ were prepared in an inert atmosphere arc furnace with appropriate care taken to compensate for the weight loss of the more volatile Sn and In. The samples were wrapped with Ta foil and were annealed at 650 °C for 2–5 days. Powdered x-ray-diffraction measurements at room temperature indicated that all samples had a cubic Cu_3Au structure and, except for $GdSn_3$, were single phase. In the case of $GdSn_3$, extra diffraction lines with very weak intensities were found and these could be indexed in terms of metallic Sn lines. The lattice constants across the series decreased linearly with increasing In concentration from a value of 4.681 Å for $GdSn_3$ to 4.611 Å for $GdIn_3$, in agreement with Vegard's law. The magnetic susceptibility was measured from 1.8 to 400 K using a Quantum Design superconducting quantum interference device magnetometer. The specific heat was measured using a quasiadiabatic heat pulse method with a He^4 specific-heat probe for the temperature interval 1.2 K $\leqslant T \leqslant$ 25 K and a closed-cycle refrigerator system for higher temperatures. The Mössbauer samples were prepared by mixing 400 mesh sieved polycrystalline powder with epoxy, to form a disk. A $Ca^{119}SnO_3$ source was used in conjunction with an electromechanical velocity transducer operating in a triangular velocity mode. The temperature dependence of the Mössbauer spectra was measured from 4.2 to 300 K using an adjustable He-flow cryostat and from 1.5 to 4.2 K by pumping liquid ^{4}He.

RESULTS AND DISCUSSION

The temperature dependence of the magnetic susceptibility $\chi(T)$ for the $Gd(Sn_{1-x}In_x)_3$ samples with $x=0.0$, 0.265, 0.55, 0.58, 0.80, and 1.0 is shown in Fig. 1. For the $x=0.0$ sample ($GdSn_3$) a typical cusplike antiferromagnetic transition is seen, and the Néel temperature T_{N1} is taken to be 31 K, the temperature where the cusp occurs. For other samples with $0 \leqslant x \leqslant 0.25$, $\chi(T)$ exhibits a similar behavior (not shown). For $x=0.265$, $\chi(T)$ shows not only an antiferromagnetic transition at T_{N1}, but also a second anomaly at a

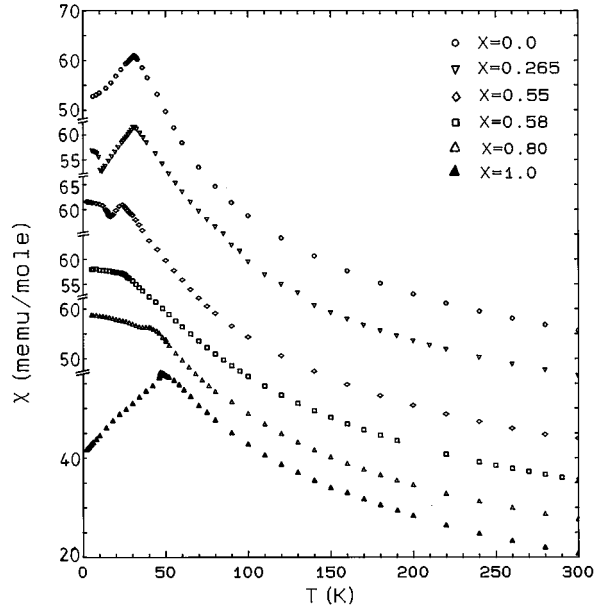

FIG. 1. The magnetic susceptibility vs temperature of $Gd(Sn_{1-x}In_x)_3$ with $x=0.0$, 0.265, 0.55, 0.58, 0.80, and 1.0.

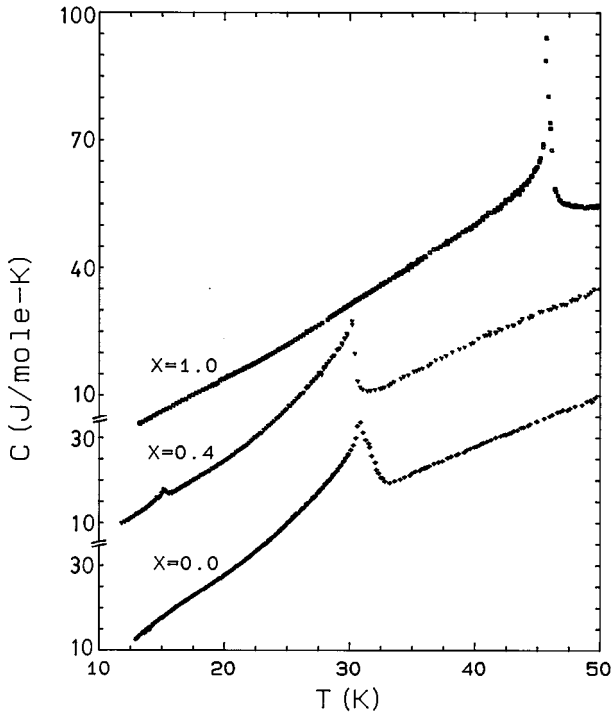

FIG. 2. The specific heat vs temperature of $Gd(Sn_{1-x}In_x)_3$ with $x=0.0$, 0.40, and 1.0.

lower temperature, which looks like an inverted cusp. This lower temperature anomaly indicates that the sample undergoes a second magnetic transition. We define T_{N2} as the temperature of the inverted cusp. We have ruled out the possibility that this second transition is due to impurities in the sample, as will be discussed later in connection with the specific-heat and Mössbauer measurements. The two magnetic transition behavior occurs for In concentrations in the range $0.265 \leqslant x \leqslant 0.565$. As x increases in this range, $(T_{N1}-T_{N2})$ lessens. Finally when the In concentration increases to $x=0.58$, the first and second magnetic transitions coalesce to the same temperature (~22 K) and become a single magnetic transition. $\chi(T)$ for the $x=0.58$ sample remains almost constant below 22 K showing neither the cusp nor the inverted cusp behavior (see Fig. 1). Our Mössbauer results, which will be presented later in this paper, suggest that this low-temperature saturation may be due to a canting of the Gd moment. As the In concentration is increased in the range $0.58 \leqslant x \leqslant 1$, T_N increases from 22 to 47 K. In the range $0.8 \leqslant x \leqslant 1$ there is a gradual evolution of $\chi(T)$ from an essentially constant χ below T_N for $x=0.8$ to a pronounced cusp behavior for $x=1.0$.

At temperatures $T > T_{N1}$, the $\chi(T)$ curves for all samples show a Curie-Weiss behavior, i.e., $\chi = C/(T-T^*)$, and their effective paramagnetic moments, which can be extracted from the Curie constant, have values of approximately $8\mu_B$, across the entire series from $x=0.0$ ($GdSn_3$) to $x=1.0$ ($GdIn_3$). Note that this value of $8\mu_B$ can be attributed entirely to the Gd ions, and is consistent with theoretical calculations.[10]

Figure 2 shows the temperature dependence of the specific heat $C(T)$ of $Gd(Sn_{1-x}In_x)_3$ for $x=0.0$, 0.40, and 1.0. A specific-heat anomaly which is associated with the magnetic ordering transition is clearly evident for the case of the pure $GdSn_3$. The T_{N1} value obtained from the $C(T)$ data is consistent with that measured from the $\chi(T)$ curve. Two anomalies appear in the specific-heat data for samples with In concentrations in the range $0.265 \leqslant x \leqslant 0.565$ which is consistent with the $\chi(T)$ behavior just discussed. The specific-heat behavior for the $x=0.40$ sample shown in Fig. 2 is representative of the behavior seen for samples in the concentration range. The lower magnetic transition temperature T_{N2}, extracted from the lower temperature specific-heat anomaly, is the same as that obtained from $\chi(T)$. Note that the x-ray measurements which indicate a single phase and the measurement of a sizeable lower temperature specific-heat anomaly, confirm that the second transition is a bulk property, i.e., an intrinsic feature of these materials and not the result of impurities. As the In concentration increases, i.e., $0.58 \leqslant x \leqslant 1.0$, the $C(T)$ measurements show only one specific-heat anomaly again consistent with $\chi(T)$ results.

T_{N1} and T_{N2} for $Gd(Sn_{1-x}In_x)_3$ obtained from both the magnetic susceptibility and specific-heat measurements are plotted in Fig. 3. Several interesting features are shown in this figure. First, T_{N1} shows an oscillatory behavior across the series. This type of variation has been observed for properties other than T_{N1} for isostructural rare-earth compounds,[11,12] e.g., the superconducting transition temperature, the thermopower, and the electronic specific-heat coefficient for $La(Sn_{1-x}In_x)_3$, and has been attributed to a band-structure effect arising from the mixing of the $5d$ electron from the rare-earth ions and the s and p bands of the Sn and In. The oscillatory behavior in T_{N1} was also seen in the $Nd(Sn,In)_3$ system, and was explained[6] by the indirect Ruderman-Kittel-Kasuga-Yosida mechanism in which free conduction electrons mediate the isolated $4f$ electron interaction. Second, the lower temperature magnetic transition appears between the two local minima of T_{N1} vs In concentration (i.e., In concentrations from $x=0.265$ to $x=0.565$). Third, T_{N2} also shows an oscillatory variation, following a similar trend to that of T_{N1}, and finally merging with T_{N1} in

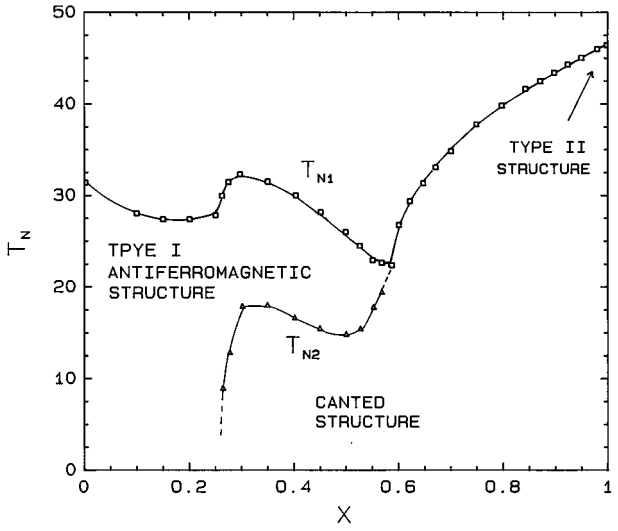

FIG. 3. The magnetic transition temperatures T_{N1} and T_{N2} (see definitions in the text) as function of In concentration x across the series from $GdSn_3$ ($x=0.0$) to $GdIn_3$ ($x=1.0$).

the vicinity of $x=0.58$. To be certain of the range of In concentrations and temperatures for the second transition, we have measured the magnetic susceptibility down to 1.8 K and the specific heat down to 1.2 K, as well as the Mössbauer spectra down to 1.6 K for all samples studied here, and these results give no indication of a second magnetic ordering transition for $0.0 \leqslant x \leqslant 0.25$ and $0.58 \leqslant x \leqslant 1.0$.

In order to determine the magnetic structure of $Gd(Sn_{1-x}In_x)_3$, we have carried out measurements of the temperature dependence of the ^{119}Sn Mössbauer spectra across the series. The spectra at various temperatures for the $x=0.20$ are shown in Fig. 4. It should be noted that we focus attention on the spectra of the $x=0.20$ sample, instead of those of pure $GdSn_3$, because the pure $GdSn_3$ samples show a small amount of Sn-metal precipitation typical of pure Cu_3Au compounds containing Sn.[13] The room-temperature spectrum shown in Fig. 4(a) exhibits the usual quadrupole splitting ($\Delta E \approx e^2qQ$) due to the tetragonal symmetry of the Sn sites in the Cu_3Au structure. All room-temperature spectra across the series from $x=0.0$ to $x=0.98$ (2% ^{119}Sn in $GdIn_3$) show a similar quadrupole splitting. The quadrupole splitting parameter increases monotonically from 0.465 mm/s for $x=0.0$ to 0.613 mm/s for $x=0.98$ indicating an increase in the electric-field gradient at the Sn sites, as the lattice constant decreases. The isomer shift measured relative to the $Ca^{119}SnO_3$ source decreases with increasing In concentration from 2.298 mm/s for $x=0$ to 2.132 mm/s for $x=0.98$, indicating a decrease in the s-electron density at the Sn nuclei.

The spectrum stays essentially the same down to 30 K, the lowest temperature above T_{N1} for the data of Fig. 4, i.e., $T_{N1}=27.5$ K for $x=0.20$ [see Fig. 4(b)]. Figure 4(c) shows that a distinct magnetic hyperfine field can be observed at $T=26$ K. The hyperfine field increases with decreasing temperature [see the sequence from 4(c) to 4(e) for $T=26$ K to 4.2 K, respectively]. From the plot of the hyperfine field vs temperature one can determine T_N, which is defined as the temperature in which the hyperfine field goes to zero; a value of about 27.5 K obtained for this sample ($x=0.20$) is consistent with that from the $\chi(T)$ and $C(T)$ measurements. The fits of the Mössbauer spectra at various temperatures below T_{N1} for the $x=0.20$ sample and for samples with In concentrations $0.0 \leqslant x \leqslant 0.25$ (after subtracting the contribution of the small amount of Sn-metal impurity on the Sn-rich side) show that about 2/3 of the Sn ions see no hyperfine field [central dips in curves 4(c), 4(d), and 4(e)] and about 1/3 of the Sn ions see a net hyperfine field (outer splitting). In the presence of a magnetic hyperfine field H_f and an electric-field gradient ΔE, the electric-field gradient can be expressed as: $\Delta E \approx e^2qQ(3\cos\alpha - 1)/2$, where α is the angle between H_f and ΔE. The quadrupole splitting parameter obtained from the hyperfine-split spectra below T_{N1} for $0.0 \leqslant x \leqslant 0.25$ is about 1/2 of that at temperatures above T_{N1}, indicating that the magnetic hyperfine field is perpendicular to the electric-field gradient ($\alpha=\pi/2$). Hence, the magnetic structure of these materials ($0.0 \leqslant x \leqslant 0.25$) corresponds to a type-I antiferromagnetic ordering [see Fig. 5(a)] which consists of the Gd moments in the (100) planes being aligned in the same direction within the planes, but alternating directions in adjacent (100) planes. However, the orientation of the moments within the (100) plane cannot be deduced from these spectra since the electric-field gradient is axially symmetric. Sn ions are located at the face centers of the cubic cell. It can be seen from Fig. 5(a) that 1/3 of the Sn ions see a net hyperfine field, namely the Sn ions at the centers of the top and bottom faces. On the other hand, 2/3 of the Sn ions see zero hyperfine field due to the cancellation of the fields from the four Gd ions, namely the Sn ions at the centers of the left, right,

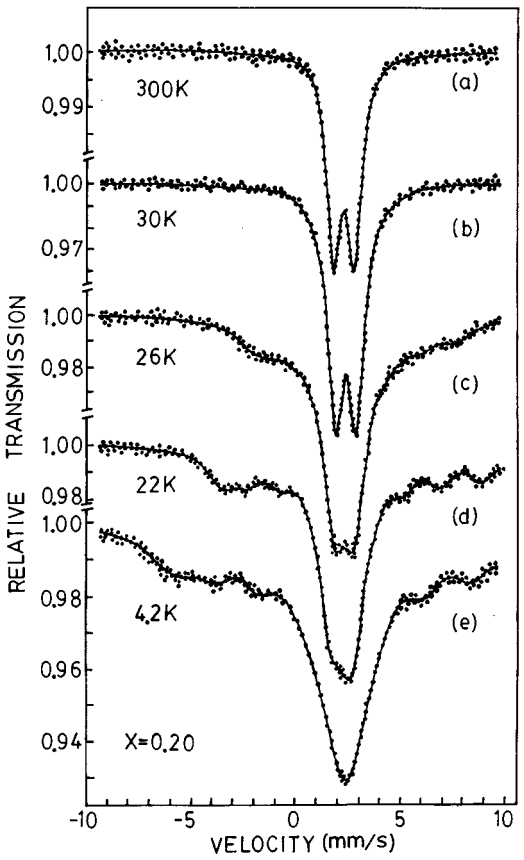

FIG. 4. The Mössbauer spectra for the $x=0.20$ sample at (a) room temperature, (b) 30 K, (c) 26 K, (d) 22 K, and (e) 4.2 K.

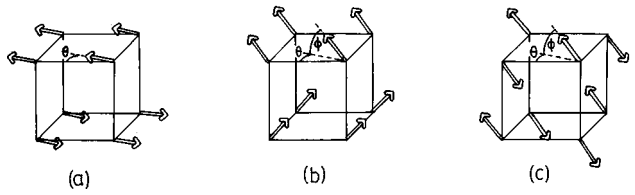

FIG. 5. The proposed magnetic structures for the $Gd(Sn_{1-x}In_x)_3$ system: (a) type-I antiferromagnetic structure, (b) canted antiferromagnetic structure, and (c) type-II antiferromagnetic structure. Note that both θ and ϕ cannot be determined from polycrystalline samples.

front, and back faces of the cell.

As we have seen previously, samples with In concentrations in the range of $0.265 \leqslant x \leqslant 0.565$ show two magnetic transitions at T_{N1} and T_{N2}. The Mössbauer measurements of such samples are typified by the $x=0.4$ sample for which we show spectra measured at various temperatures in Fig. 6. The spectrum for $T=35$ K, shown in Fig. 6(a), is similar to the room-temperature spectrum. At $T=28$ K, which is slightly below the first transition, $T_{1N}=30$ K, a hyperfine field is clearly evident [Fig. 6(b)]. At $T=18$ K, which is just slightly above the second transition, $T_{N2}=17$ K, the spectrum [Fig. 6(c)] is similar to the spectra shown in Figs. 4(c), 4(d), and 4(e) for the $x=0.20$ sample. Again, based on the same argument mentioned previously the magnetic structure at temperatures $T_{N2}<T<T_{N1}$ corresponds to the type-I antiferro-

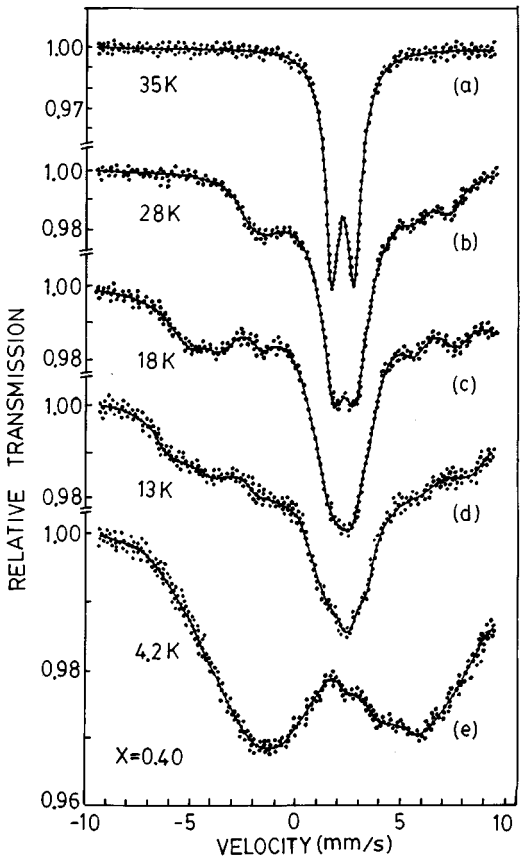

FIG. 6. The Mössbauer spectra for the $x=0.40$ sample at (a) 35 K, (b) 28 K, (c) 18 K, (d) 13 K, and (e) 4.2 K.

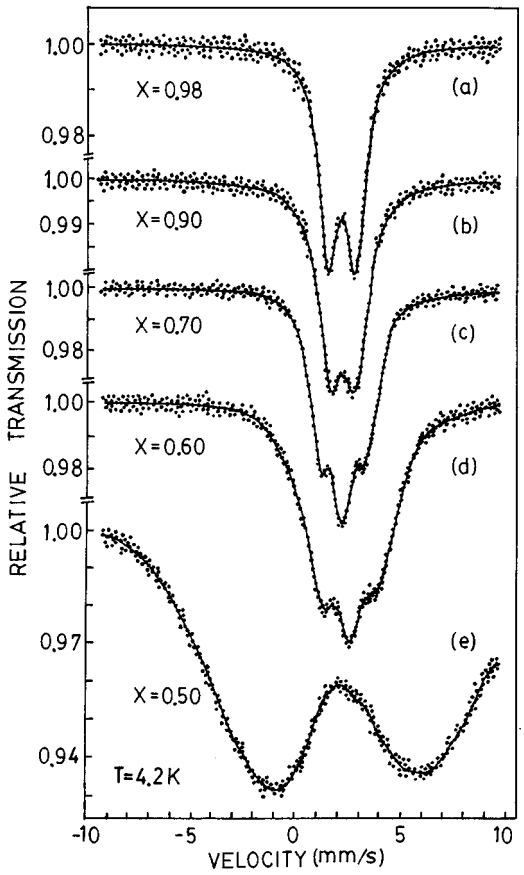

FIG. 7. The Mössbauer spectra at $T=4.2$ K for $Gd(Sn_{1-x}In_x)_3$ with (a) $x=0.98$, (b) $x=0.90$, (c) $x=0.70$, (d) $x=0.60$, and (e) $x=0.50$.

magnetic structure. For $T<T_{N2}$ [see Fig. 6(d) for $T=13$ K], the central part of the spectrum starts to split, and this implies that the 2/3 of the Sn ions, which see no hyperfine field in the type-I structure, now begin to experience a magnetic hyperfine field, which increases in magnitude as the temperature is lowered. By 4.2 K, the spectrum is seen to consist of two very broad dips [Fig. 6(e)], which represent a smearing of hyperfine fields. This is an additional confirmation that the second magnetic transition is a bulk property and is not due to impurities. From the observations that the $x=0.4$ sample is antiferromagnetic (type-I) at $T_{N2}<T<T_{N1}$ and that all Sn ions see a range of hyperfine fields below T_{N2}, we propose that the magnetic structure of this compound for $T<T_{N2}$ is a canted antiferromagnetic state,[14,15] in which the directions of the magnetic moments change with temperature [see Fig. 5(b)]. The inverted cusplike behavior in $\chi(T)$ for $T<T_{N2}$ for the $0.265 \leqslant x \leqslant 0.565$ samples is also consistent with the proposed magnetic structure. Neutron-diffraction measurements are difficult to perform on this system due to high neutron absorption of Gd. Mössbauer measurements under high magnetic fields are underway, and can presumably provide more information to clarify this issue.

The Mössbauer spectrum for $x=0.98$, $Gd(^{119}Sn_{0.02}In_{0.98})_3$, at $T=4.2$ K is shown in curve 7(a). A quadrupole doublet is observed at 4.2 K, slightly broadened as compared with that measured at room temperature. This zero (or near zero) net magnetic hyperfine field at tempera-

tures below $T_{N1}=46$ K results from the cancellation of the transferred magnetic hyperfine field contributions due to the Gd moments at all Sn sites. Hence this implies that the magnetic moments of the Gd ions in this sample should be aligned in the same directions within (111) planes, and in the opposite direction in the adjacent planes. This constitutes the so called type-II antiferromagnetic structure [see Fig. 5(c)] for Cu_3Au fcc compounds.[5]

The spectrum shown in Fig. 7(e) for the $x=0.50$ sample at $T=4.2$ K is similar to that shown in Fig. 6(e) for $x=0.40$. Both the $x=0.40$ and $x=0.50$ samples have two magnetic transitions. Curves 7(b), 7(c), and 7(d) are the Mössbauer spectra at $T=4.2$ K for $x=0.90$, 0.70, and 0.60, respectively. These samples have only one magnetic transition. The hyperfine field is significantly reduced from $x=0.50$ to $x=0.60$ and decreases further with increasing In concentration from $x=0.60$ to $x=0.90$. Moreover, these spectra for $x=0.60$, 0.70, and 0.90 are completely different from those shown in Fig. 4(c), 4(d), and 4(e) for the $x=0.20$ samples and the spectrum shown in Fig. 7(a) for the $x=0.98$ sample. Therefore the magnetic structure below T_{N1} for $x=0.60$, 0.70, and 0.90 is neither type-I nor type-II antiferromagnetic ordering. Although the fit to the spectra of these samples has a large uncertainty due to the smaller magnitude of the hyperfine field, it seems to indicate that in this region of In concentrations Sn ions see either one or two hyperfine fields. As mentioned earlier, $\chi(T)$ shows a saturation behavior instead of a cusplike for the $0.58\leqslant x\leqslant 0.90$ samples. Hence, we suggest that the magnetic structure for $0.58\leqslant x\leqslant 0.90$ below T_{N1} could be a different canted antiferromagnetic structure that preceeds the transition from a type-II antiferromagnetic ordering for $GdIn_3$ to a canted antiferromagnetic structure for samples with In concentrations $0.265\leqslant x\leqslant 0.565$ at $T<T_{N2}$.

We have shown an oscillatory T_{N1} variation across the series in $Gd(In_{1-x}Sn_x)_3$ from measurements of the magnetic susceptibility, specific heat, and Mössbauer spectra. In addition, a second magnetic ordering transition emerges at temperatures well below T_{N1} in the range of In concentrations $0.265\leqslant x\leqslant 0.565$. From the Mössbauer spectra and the $\chi(T)$ measurements, we infer that the magnetic structure on the Sn-rich side ($0.0\leqslant x\leqslant 0.25$) and for $0.265\leqslant x\leqslant 0.565$ in the temperature interval $T_{N2}<T<T_{N1}$ is of type-I antiferromagnetic ordering. It is of type-II structure on the very rich In side ($x\rightarrow 1.0$). It could be a canted antiferromagnetic state for $0.265\leqslant x\leqslant 0.565$ with $T<T_{N2}$ and for $0.565<x<1.0$ with $T<T_{N1}$.

ACKNOWLEDGMENT

We acknowledge support from the Materials Research Center at Temple University.

[1] L. E. DeLong, R. P. Guertin, and S. Foner, Solid State Commun. **32**, 833 (1979).
[2] D. Kim and P. M. Levy, J. Magn. Magn. Mater. **27**, 257 (1982).
[3] J. Lawrence, Phys. Rev. B **20**, 3770 (1979).
[4] L. W. Zhou, C. L. Lin, J. E. Crow, S. Bloom, R. P. Guertin, and S. Foner, Phys. Rev. B **34**, 483 (1986).
[5] J. P. Sanchez, J. M. Friedt, G. K. Shenoy, A. Percheron, and J. C. Achard, J. Phys. C **9**, 2207 (1976).
[6] T. Hirdoka and K. Kamihira, J. Magn. Magn. Mater. **87**, 209 (1990).
[7] *Physics of Highly Correlated Electron Systems*, edited by J. O. Willis, J. D. Thompson, R. P. Guertin, and J. E. Crow (North-Holland, Amsterdam, 1990); also see, Physica B **163**, (1990).
[8] Tan Yuen, C. L. Lin, T. Mihalisin, and N. Bykovetz, J. Appl. Phys. **70**, 5995 (1991).
[9] K. H. J. Buschow, H. W. de Wijn, and A. M. van Diepen, J. Chem. Phys. **50**, 137 (1969).
[10] See, for example, C. Kittel, *Introduction to Solid State Physics* (Wiley, New York, 1996).
[11] W. D. Grobman, Phys. Rev. B **5**, 2924 (1972).
[12] E. E. Havinga, H. Damsma, and M. H. van Maaren, J. Phys. Chem. Solids **31**, 2653 (1970).
[13] I. R. Harris and G. V. Raynor, J. Less Common Met. **9**, 7 (1965).
[14] J. S. Kouvel and J. S. Kasper, J. Phys. Chem. Solids **24**, 529 (1963).
[15] P. Morin and A. de Combarieu, Solid State Commun. **17**, 975 (1975).